Available online at www.sciencedirect.com
ScienceDirect
Trans. Nonferrous Met. Soc. China 25(2015) 2587−2593
Transactions of Nonferrous Metals Society of China
www.tnmsc.cn

Effect of Al-deposition on erosion resistance of plasma sprayed thermal barrier coating

Xiao-feng ZHANG[1,2], Ke-song ZHOU[1,2], Shu-juan DONG[3], Wei XU[2], Jin-bing SONG[2], Min LIU[2]

1. School of Materials Science and Engineering, South China University of Technology, Guangzhou 510640, China;
2. Institute of New Materials, Guangzhou Research Institute of Non-ferrous Metals, Guangzhou 510650, China;
3. IRTES-LERMPS Laboratory, Université de Technologie de Belfort-Montbéliard, Belfort Cedex 90010, France

Received 31 October 2014; accepted 28 December 2014

Abstract: A columnar Al film was firstly deposited on the top of 7%Y_2O_3−stabilized zirconia (7YSZ) ceramic coating in thermal barrier coating (TBC) system by magnetron sputtering. A vacuum treatment was then carried out at 700 °C for 1 h and 900 °C for 5 h to improve the erosion resistance of Al-deposited TBC. A α-Al_2O_3 layer was in situ synthesized on the top of 7YSZ coating via vacuum heat treatment. The microstructure evolution of Al-deposited TBC illustrated that a loose surface-layer and a dense sub-layer formed on the top of 7YSZ coating after vacuum treatment. The phase structures of the as-sprayed TBC and the Al-deposited TBC after vacuum heat treatment were characterized by X-ray diffraction (XRD) and transmission electron microscope (TEM) assisted with focused ion beam (FIB). Particulate erosion resistances of the as-sprayed TBC and treated TBC were compared at room temperature. In addition, erosion mechanism and schematic diagram were proposed. The results show that the Al-deposited TBC after vacuum heat treatment has better particulate erosion resistance than the as-sprayed one.
Key words: thermal barrier coating; 7%Y_2O_3−stabilized zirconia (7YSZ); erosion resistance; in situ synthesis; α-Al_2O_3

1 Introduction

Thermal barrier coatings (TBCs) have been widely used in the high-temperature components of aircraft and industrial gas-turbine engine [1,2]. The structure of TBCs generally consists of a thermally insulating ceramic top coating and an intermediate oxidation resistant metallic bond coating. The top ceramic coating is typically made of yttria−stabilized zirconia for low thermal conductivity and high thermal-expansion coefficient. The bond coating is typically made of MCrAlY (M: Ni, Co and Ni+Co) for its good oxidation resistance [3]. The failure mechanism of TBCs is very complex, including oxidation of bond coating, corrosion of ceramic coating, etc. Especially, particulate erosion is also an important degradation aspect [4,5]. Particulate erosion of TBCs is generally caused by the action of sliding or impact of solids, liquids or a combination of these elements [6,7].

In the last decades, the erosion failure mechanism of TBCs attracted many researchers, such as MARASHALL and EVANS [8], CHEN et al [9], and WELLMANA et al [10]. It is well recognized that erosion rate of TBCs is affected by many factors which could be broadly classified into three types: impingement, particle and materials variables. The impingement variables mainly consist of particle velocity, particle concentration and angle of incidence. The particle variables include particle shape, size and hardness, etc. Materials variables involve target material properties, such as hardness and porosity [11,12]. The majority of the derived relationship for the erosion rate (v) is of the Eq. (1) given by JANOS et al [5].

$$v=10^{10}a\ H_t^{-b} \tag{1}$$

where v is the erosion rate, H_t is the Vickers microhardness of the target material (TBC), a and b are two constants (>0). So, the higher the TBCs' microhardness is, the lower the erosion rate is.

Up to now, a lot of methods were proposed to improve the erosion resistance of TBCs, such as, laser glazing and remelting of ceramic coating [13,14], doping of rare earth material like gadolinia [15]. In this work,

Foundation item: Project (2012CB625100) supported by the National Basic Research Program of China; Project (2012AA03A512) supported by the National High-tech Research and Development Program of China
Corresponding author: Ke-song ZHOU; Tel: +86-20-37238263; Fax: +86-20-37238531; E-mail: kszhou2004@163.com
DOI: 10.1016/S1003-6326(15)63879-1

an innovative approach was presented. Firstly, Al was deposited on the surface of 7YSZ coating by direct current circular magnetron sputtering. And then vacuum heat treatment (at 700 °C for 1 h and 900 °C for 5 h) was carried out in order to in situ synthesize a α-Al_2O_3 overlay through the reaction of Al and ZrO_2 on the top of 7YSZ coating. The surface microhardness and porosity of the treated TBCs were investigated. It is expected to improve the particulate erosion resistance of TBC.

2 Experimental

2.1 Sample preparation

The superalloy K4169 sheet with sizes of *d*25.4 mm×5 mm was used as the substrate material. The material used for bond coating was commercial NiCoCrAlYTa powders. Agglomerated and sintered ZrO_2−7% Y_2O_3 (7YSZ) powders as top coating materials were provided by H. C. Starck. The composition of these materials is presented in Table 1. Prior to the deposition of bond coating, the substrates were degreased and cleaned with petrol and ethanol, followed by grit blasting with alumina under 0.2 MPa. Both the bond and ceramic coatings were prepared by atmospheric plasma spray (APS, MF−P1000, GTV, Germany). The thicknesses of bond and top ceramic coatings were about 100 and 250 μm, respectively. Then, Al film with a thickness of 15 μm was deposited on the surface of 7YSZ coating by direct current circular magnetron sputtering (J−1250, Jingzhou Industrial Coating, China). Before deposition of Al film, the TBC surface was polished by diamond paste with a size of 2.5 μm (*D*50) for 30 min. For the magnetron sputtering, Al target (99.99%) was used and the direct current, voltage and pressure were set at 3 A, 150 V and 5×10^{-3} Pa, respectively. Then, Al-deposited TBC samples were put in a closed vacuum tube (about 2×10^{-3} Pa) for heat treatment at 700 °C for 1 h and continuously treated at 900 °C for 5 h.

Table 1 Information of powder and substrate material

Material	Purpose	Composition/%	Particle size/μm	Manufacturer
7YSZ powder	Ceramic coating	93ZrO_2−7Y_2O_3	15−45	H. C. Starck, AMPERIT^{TM} 827
NiCoCrAlYTa powder	Bond coating	22Co−19Cr−7.5Al−0.4Y−3.5Ta−rest Ni	15−45	Sulzer-Metco Amdry 997
Nickel-based superalloy K4169	Substrate	52 Ni−18.4Cr−5.3Nb−3.05Mo−rest Fe, Al	−	Antai Tec. Co., Ltd.

2.2 Particulate erosion tests

Particulate erosion tests were performed on the erosion experiment equipment which was self-modified from the sand-blasting machine, as schematically illustrated in Fig. 1. Compressed air (0.2 MPa) was used for the power, which sprayed angular Al_2O_3 particles (about 100 μm) on the surface of TBC samples. And the erosion angle and distance were 90° and 20 cm, respectively. The erosion resistances of as-sprayed and treated TBCs were compared through the eroded mass loss, which was obtained by weighing the sample per 15 s during erosion test using a precision electronic balance with 1×10^{-4} g.

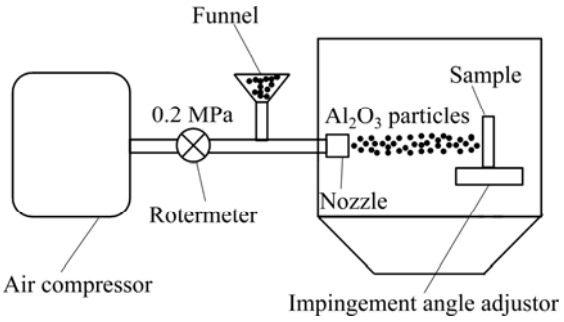

Fig. 1 Schematic diagram of sand-blasting erosion tester

2.3 Characterization of TBC

The cross-sectional microstructures of as-sprayed and Al-deposited TBCs after vacuum heat treatment were characterized by field emission-scanning electron microscope (FE-SEM, Nova-Nono430, FEI, Holland). Phase structures of both TBCs were analyzed by X-ray diffraction (XRD, D8-Advance, Bruker) with a step of 0.02°. Moreover, phase structures of the 7YSZ coatings with a α-Al_2O_3 overlay were studied by transmission electron microscope (TEM, JEM2100F, JEOL, Japan) assisted with focused ion beam (FIB, SMI3050MS2, SII, Japan). The surface microhardness of both TBCs before and after polishing was measured based on 10 values by Vickers indentation test (MH−5, Everone, China) with a load of 300 g for 15 s. Besides, the cross-sectional microstructures of as-sprayed and treated TBCs after erosion test were characterized by FE-SEM.

3 Results and discussion

3.1 Microstructure and phase analysis of as-sprayed and Al-deposited TBC

Figure 2 shows the surface and cross-sectional morphologies of the as-sprayed TBC. It can be found that the surface of as-sprayed TBC exhibits a lot of vertical cracks, which is a typical characterization of plasma-sprayed ceramic coatings (Fig. 2(a)). From the cross-sectional image of the as-sprayed TBC, it can be seen that the thicknesses of bond coating and ceramic coating are about 100 and 250 μm, respectively (Fig. 2(b)).

Figure 3 shows the SEM images of the Al-sputtered TBC before vacuum treatment. A columnar Al film (about 15 μm in thickness) forms on the surface of TBC. After vacuum treatment at 700 °C for 1 h and continuously at 900 °C for 5 h, a mixed surface morphology can be observed with loose and dense layers, as shown in Fig. 4(a). The cross-sectional image (Fig. 4(b)) confirms the presence of loose surface-layer on the top of TBC. The magnified image of marked area in Fig. 4(b) presents that a dense sub-layer forms at the interface between loose layer and ceramic coating, as shown in Fig. 4(c).

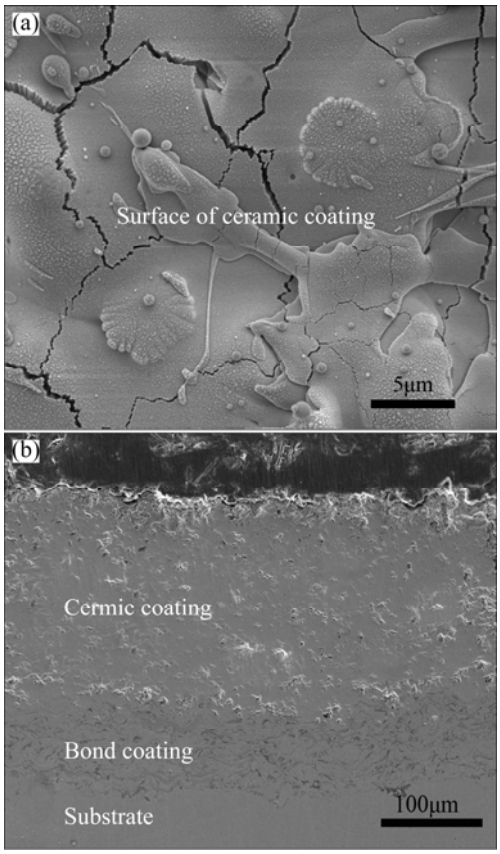

Fig. 2 SEM images of as-sprayed TBC: (a) Surface; (b) Cross section

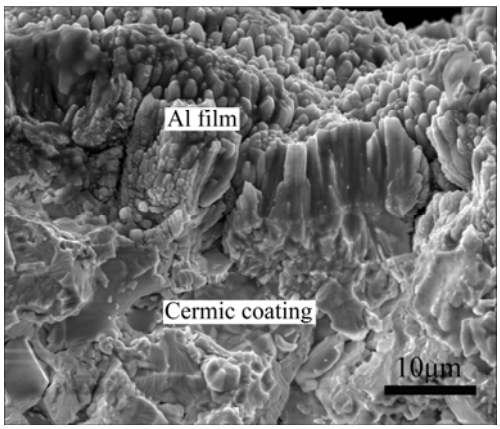

Fig. 3 SEM images of columnar Al film deposited by magnetron sputtering on ceramic coating before vacuum treatment

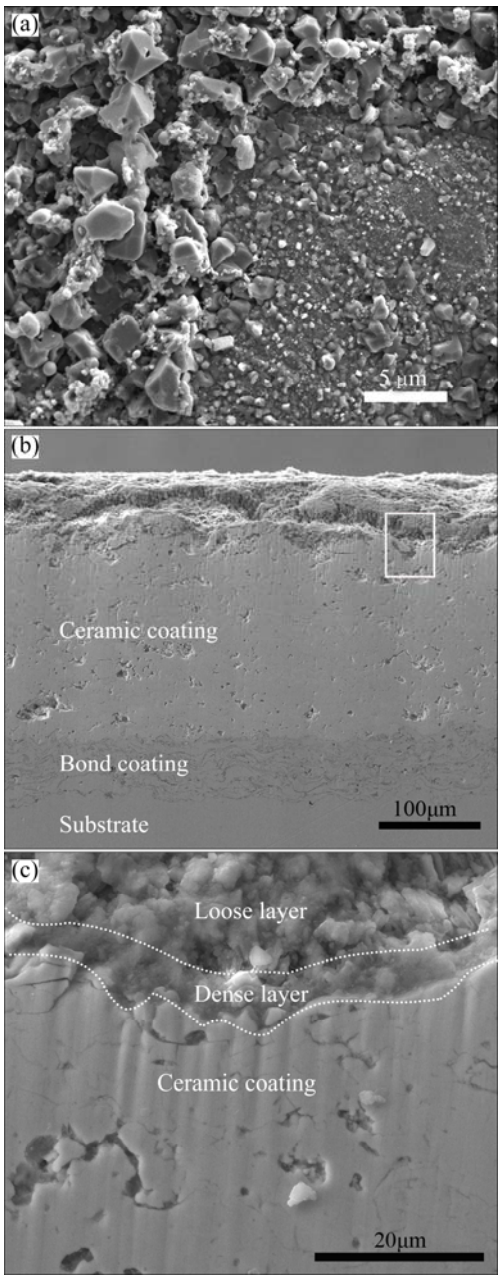

Fig. 4 SEM images of Al-deposited TBC after vacuum treatment at 700 °C for 1 h and continuously at 900 °C for 5 h: (a) Surface; (b) Cross section; (c) Frame magnification of marked area in (b)

Phase transformations of the as-sprayed and Al-deposited TBCs after vacuum heat treatment were analyzed by XRD, as shown in Fig. 5. The as-sprayed TBC is mainly composed of C-ZrO_2 and t'-ZrO_2 phases (Fig. 5(a)), while the Al-deposited and vacuum-treated TBCs consist of α-Al_2O_3, Al_3Zr and ZrO_2 (Fig. 5(b)). The α-Al_2O_3 and Al_3Zr phases result from in situ synthesis of Al and ZrO_2 at high temperatures [16,17].

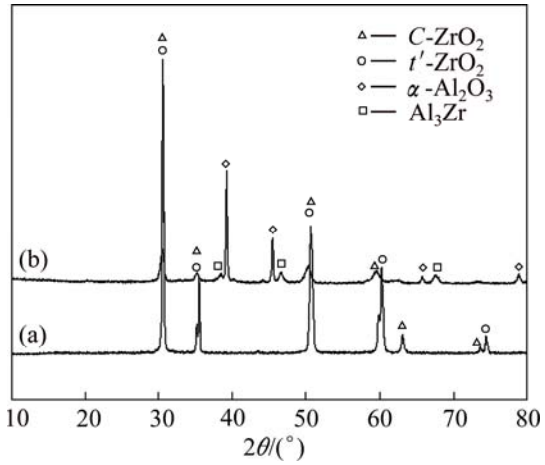

Fig. 5 XRD patterns of as-sprayed (a) and Al-deposited TBCs after vacuum treatment at 700 °C for 1 h and continuously at 900 °C for 5 h (b)

According to Refs. [18,19], the ΔG_T^{Θ} of Reaction (2) is less than 0 when the temperature is lower than 3232 K.

$$13Al+3ZrO_2 \rightarrow 2\alpha\text{-}Al_2O_3+3Al_3Zr \quad (2)$$

The treatment temperatures (700 °C for 1 h and 900 °C for 5 h) in this work meet the reaction condition. It is thus reasonable that the top layer of vacuum-treated TBC consists of α-Al_2O_3 and Al_3Zr as well as ZrO_2. The formation of α-Al_2O_3 on the top of 7YSZ coating is expected to improve the erosion resistance of TBC. Besides, the simultaneous formed Al_3Zr phase is an intermetallic compound with good fracture toughness, which could also contribute to the improvement in the erosion resistance. In addition, it is recognized that Al_3Zr phase has high melting temperature, good physical and chemical stability [20].

3.2 Comparison of erosion resistance

Figure 6 shows the room temperature erosion results of the as-sprayed and vacuum-treated TBCs. Before the erosion time of 60 s, the eroded mass loss of the vacuum-treated TBC is higher than that of the as-sprayed one due to the presence of loose surface-layer on the top of 7YSZ coating. The measured surface microhardness of porous loose layer ($HV_{0.3}$ 459, see Table 2) is lower than that of the as-sprayed TBC ($HV_{0.3}$ 568). It is thus reasonable that the erosion rate of the treated TBC is lower than that of the as-sprayed one based on Eq. (1). Subsequently, there is a steady range between 60 and 90 s, due to the presence of a dense sub-layer at the interface between loose surface-layer and ceramic coating. The dense sub-layer has a higher surface microhardness ($HV_{0.3}$ 1167) than the polished as-sprayed TBC ($HV_{0.3}$ 621). Here, the surface microhardness of the dense sub-layer was measured after polishing by diamond paste (D50, 2.5 μm) for 10 min to get rid of the loose surface-layer. However, the mass loss of treated TBC begins to decrease obviously after the erosion time of 90 s, similar to that of the as-sprayed TBC. This is because the in-situ formed dense sub-layer is eroded by Al_2O_3 particles. The microstructure of the underside coating is the same as that of the as-sprayed sample.

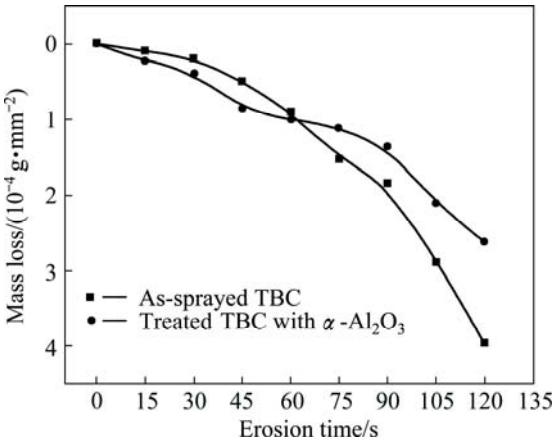

Fig. 6 Comparison of erosion resistance between as-sprayed TBC and treated TBC

Table 2 Surface microhardness of as-sprayed and treated TBCs before and after polishing

Sample	Surface microhardness of as-sprayed TBC ($HV_{0.3}$)	Surface microhardness of Al-deposited TBC after vacuum heat treatment ($HV_{0.3}$)
Before polishing	568	459
After polishing	621	1167

Figure 7 shows the cross-sectional images of as-sprayed and treated TBC samples after the erosion time of 180 s. It can be seen that the 7YSZ ceramic coating in the as-sprayed TBC sample is nearly fully eroded (Fig. 7(a)). However, there are still some ceramic coatings with a thickness of about 150 μm rest in the treated TBC sample after erosion for 180 s (Fig. 7(b)). Therefore, the Al-deposited TBC after vacuum treat treatment has better particulate erosion resistance than the as-sprayed one.

3.3 Erosion mechanism in treated TBC

The microstructural evolution of Al-deposited TBC via vacuum heat treatment is schematically presented in Fig. 8. Prior to vacuum treatment, columnar Al film is observed on porous 7YSZ ceramic coating, in which typical laminar structure can be seen with some pores and cracks (see Fig. 8(a)). During the vacuum treatment process, the Al film will translate into liquid state when heating temperature is above melting point. Then, a part

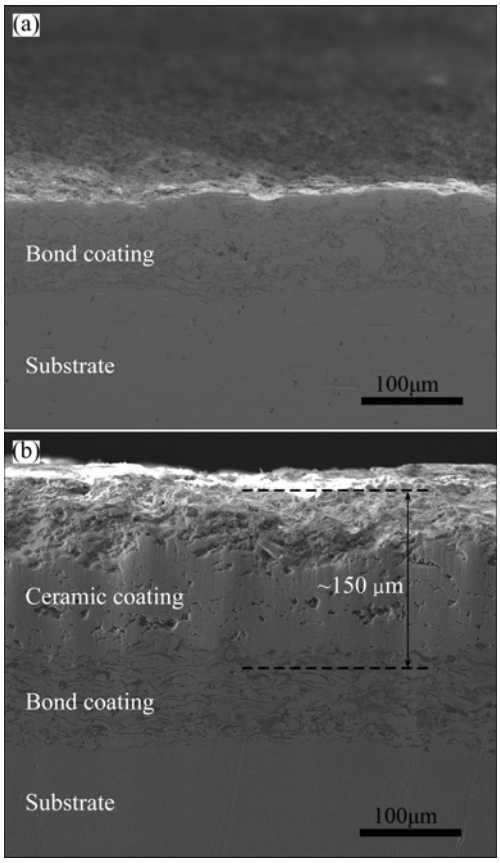

Fig. 7 Cross-sectional images of as-sprayed (a) and treated (b) TBCs after erosion time of 180 s

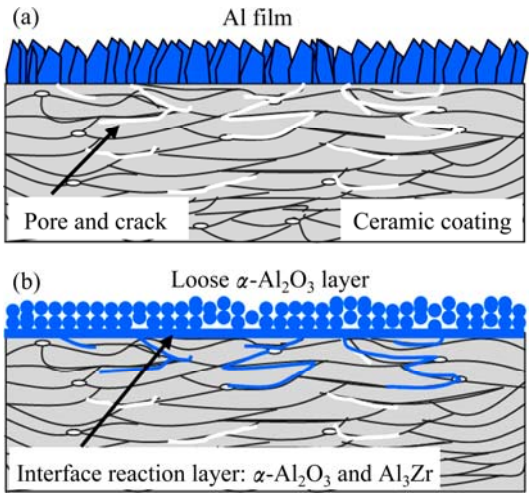

Fig. 8 Schematic diagram of Al-deposited TBC before (a) and after (b) vacuum heat treatment showing microstructure evolution

of Al will infiltrate into porous ceramic coating along surface crack by capillary force [21]. The remaining molten Al is retained on the surface of ceramic coating, where the underside Al will in situ react with ZrO_2 directly, forming a dense sub-layer, and the upside Al will form a loose surface-layer with O_2 from environment (see Fig. 8(b)). The compositions of the loose surface-layer and dense sub-layer are presented in Fig. 9. It can be found that the loose surface-layer consists of Al and O elements. While the dense sub-layer comprises mixed Al, Zr and O, whose thickness is about 4 μm. Moreover, the surface of vacuum-treated ceramic coating was analyzed by TEM, as shown in Fig. 10. Combining with the results in Fig. 10(b), it is indicated that the crack in 7YSZ ceramic coating near the interface between the dense sub-layer and the ceramic coating is filled with α-Al_2O_3 phase. The filled α-Al_2O_3 would lead to a decrease in porosity in top ceramic coating.

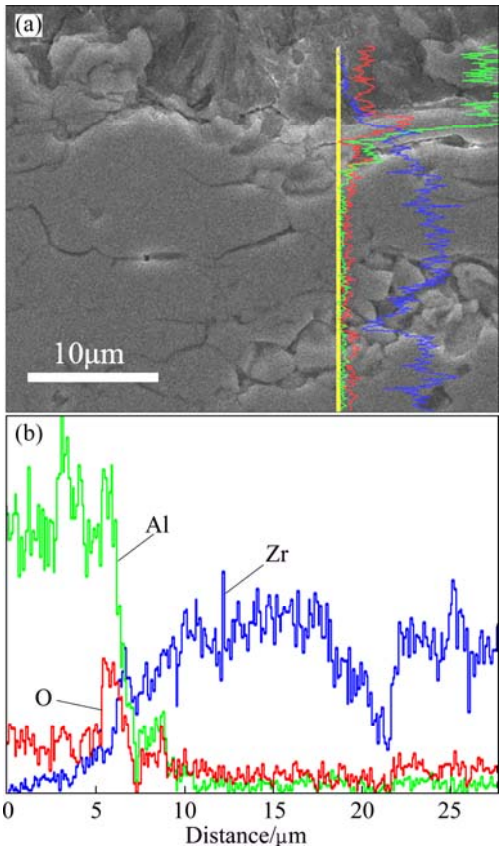

Fig. 9 SEM image of cross-section of treated TBC including loose surface-layer and dense sub-layer (a) and elemental line scanning (b)

These results agree well with the microstructure and phase analysis results mentioned above. By means of vacuum treatment, a dense sub-layer comprised α-Al_2O_3 and Al_3Zr formed between Al film and 7YSZ coating in Al-deposited TBC system due to the short diffusion path between Al and ZrO_2. And a loose surface-layer only consisted of α-Al_2O_3 formed from the remaining Al reacting with O_2 from environment. Although the loose surface-layer has a relatively high erosion rate due to the lower surface microhardness than the as- sprayed TBC, the dense layer has good erosion properties due to its high surface microhardness ($HV_{0.3}$ 1167 vs $HV_{0.3}$ 621 for

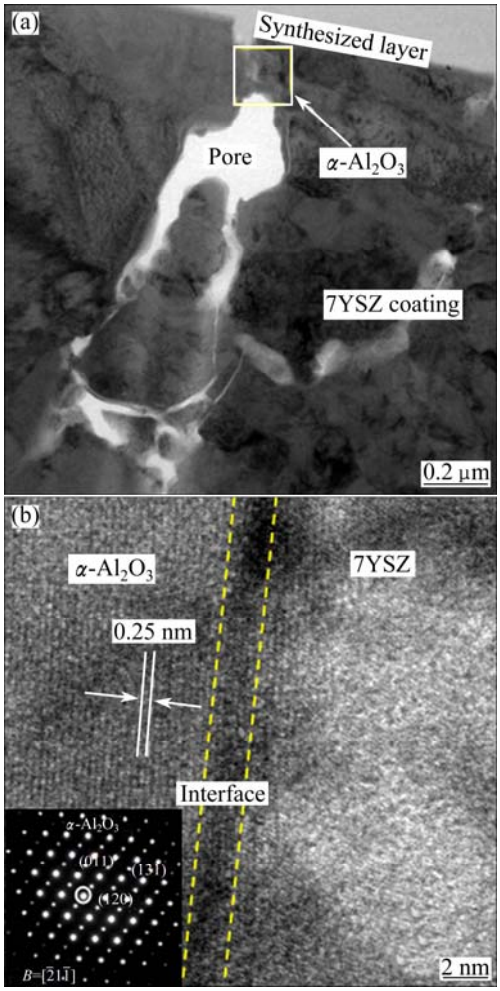

Fig. 10 Bright field TEM image of cross-section of vacuum-treated TBC showing pore in 7YSZ ceramic coating near in-situ synthesized layer (a) and HR-TEM image and SAEDP (b) of marked yellow area in (a) showing interplanar spacing of crystal plane of 0.25 nm

7YSZ in the as-sprayed TBC, see Table 2). Therefore, the Al-deposited TBC after vacuum heat treatment has better particulate erosion resistance than the as-sprayed one.

4 Conclusions

1) Columnar Al film was deposited on the TBC surface by direct current circular magnetron sputtering. The Al-deposited TBC was then vacuum-treated at 700 °C for 1 h and continuously at 900 °C for 5 h. The microstructure, phase composition and particulate erosion resistance of the Al-deposited and vacuum-treated TBCs were investigated and compared with those of the as-sprayed TBC system.

2) By means of vacuum heat treatment, the columnar Al film of the Al-deposited TBC evolved into a loose surface-layer and a dense sub-layer with a thickness of 4 μm. The dense sub-layer mainly consisted of α-Al_2O_3 and Al_3Zr which were in situ synthesized from the reaction of Al and ZrO_2 during the vacuum treatment process, and the loose surface-layer only comprised α-Al_2O_3 due to the reaction of the reminder molten Al with O_2.

3) A 7YSZ top layer with less porosity was obtained because of the pore filling by α-Al_2O_3 phases. The Al-deposited TBC after vacuum heat treatment thus exhibits better particulate erosion resistance than that of the as-sprayed one due to higher surface microhardness of the formed dense sub-layer.

References

[1] LI Chang-jiu, LI Yong, YANG Guan-jun, CHENG Xin-li. A novel plasma-sprayed durable thermal barrier coating with a well-bonded YSZ interlay between porous YSZ and bond coat [J]. J Therm Spray Technol, 2012, 21(3−4): 383−390.

[2] LIU Chun-bo, ZHANG Zhi-min, JIANG Xian-liang, LIU-min, ZHU Zhao-hui. Comparison of thermal shock behaviors between plasma-sprayed nanostructured and conventional zirconia thermal barrier coatings [J]. Transactions of Nonferrous Metals Society of China, 2009, 19(1): 99−107.

[3] LU Z, KIM M S, MYOUNG S W, LEE J H, JUNG Y G, LIM I S, JO C Y. Thermal stability and mechanical properties of thick thermal barrier coatings with vertical type cracks [J]. Transactions of Nonferrous Metals Society of China, 2014, 24(1): 29−35.

[4] ESTARIKI M R L, RAZAVI R S, EDRIS H, POURBAFRANY M, JAMALI H, GHASEMI R. Life time of new SYSZ thermal barrier coatings produced by plasma spraying method under thermal shock test and high temperature treatment [J]. Ceramics International, 2014, 40(1): 1405−1414.

[5] JANOSA B Z, LUGSCHEIDERB E, REMERB P. Effect of thermal aging on the erosion resistance of air plasma sprayed zirconia thermal barrier coating [J]. Surf Coat Technol, 1999, 113(3): 278−285.

[6] NICHOLLSA J R, DEAKINB M J, RICKERBYB D S. A comparison between the erosion behaviors of thermal spray and electron beam physical vapor deposition thermal barrier coatings [J]. Wear, 1999, 233−235(3): 352−361.

[7] WELLMANA R G, DEAKINB M J, NICHOLLSA J R. The effect of TBC morphology on the erosion rate of EB PVD TBCs [J]. Wear, 2005, 258(1−4): 349−356.

[8] MARASHALL D B, EVANS A G. Particle size distribution effects on the solid particle erosion of brittle materials [J]. Wear, 1981, 71(3): 363−373.

[9] CHEN A X, HEB M Y, SPITSBERGC I, FLECKD N A, HUTCHINSONE J W, EVANSB A G. Mechanisms governing the high temperature erosion of thermal barrier coatings [J]. Wear, 2004, 256(7−8): 735−746.

[10] WELLMANA R G, NICHOLLSA J R, MURPHYB K. Effect of microstructure and temperature on the erosion rates and mechanisms of modified EB PVD TBCs [J]. Wear, 2009, 267(11): 1927−1934.

[11] KRISHNAMUTHY N, MURALI M S, VENKATARAMAN B, MUKUNDA P G. Characterization and solid particle erosion behavior of plasma sprayed alumina and calcia-stabilized zirconia coatings on Al-6061 substrate [J]. Wear, 2012, 274−275: 15−27.

[12] WANG L, WANG Y, SUN X G, PAN Z Y, HE J Q, LI C G. Influence of pores on the surface microcompression mechanical response of

thermal barrier coatings fabricated by atmospheric plasma spray-finite element simulation [J]. Applied Surface Science, 2011, 257(6): 2238−2249.

[13] WANG Dong-sheng, TIAN Zong-jun, SHEN Li-da, LIU Zhi-dong, HUANG Yin-hui. Effects of laser remelting on microstructure and solid particle erosion characteristics of ZrO_2−7wt%Y_2O_3 thermal barrier coating prepared by plasma spraying [J]. Ceramics International, 2014, 40(6): 8791−8799.

[14] BATISTA C, PPRTINHA A, RIBEIRO R M, TEIXEIRA V, COSTA M F, OLIVEIRA C R. Surface laser-glazing of plasma-sprayed thermal barrier coatings [J]. Applied Surface Science, 2005, 247(1−4): 313−319.

[15] STEENBAKKER R J, WELLMAN R G, NICHOLLS J R. Erosion of gadolinia doped EB-PVD TBCs [J]. Surf Coat Technol, 2006, 201(6): 2140−2146.

[16] ZHU He-guo, JIA Cui-cui, LI Jian-liang, ZHAO Jun, SONG Jin-zhu, YAO Yin-qun, XIE Zong-han. Microstructure and high temperature wear of the aluminum matrix composites fabricated by reaction from Al−ZrO_2−B elemental powders [J]. Powder Technology, 2012, 217: 401−408.

[17] ZHU He-guo, MIN Jing, LI Jian-liang, AI Ying-lu, GE Liang-qi, WANG Heng-zhi. In situ fabrication of (α-Al_2O_3+Al_3Zr)/Al composites in an Al−ZrO_2 system [J]. Comp Sci Technol, 2010, 70(15): 2183−2189.

[18] ZHU He-guo, AI Ying-lu, MIN Jing, WU Qing, WANG Heng-zhi. Dry sliding wear behavior of Al-based composites fabricated by exothermic dispersion reaction in an Al−ZrO_2−C system [J]. Wear, 2010, 268(11−12): 1465−1471.

[19] MUSIL J, SKLENKA J, CERSTVY R, SUZUKI T, MORI T, TAKAHASHI M. The effect of addition of Al in ZrO_2 thin film on its resistance to cracking [J]. Surf Coat Technol, 2012, 207: 355−360.

[20] MORERE B, SHAHANI R, MAURICE C, DRIVER J. The influence of Al_3Zr dispersoids on the recrystallization of hot-deformed AA 7010 alloys [J]. Metal Mat Trans A, 2001, 32(3): 625−632.

[21] KRAMER S, YANG J, LEVI C G, JOHNSON C A. Thermochemical interaction of thermal barrier coatings with molten CaO−MgO−Al_2O_3−SiO_2 (CMAS) deposits [J]. J Am Ceram Soc, 2006, 89(10): 3167−3175.

镀铝对 7YSZ 热障涂层冲刷性能的影响

张小锋[1,2]，周克崧[1,2]，董淑娟[3]，徐 伟[2]，宋进兵[2]，刘 敏[2]

1. 华南理工大学 材料科学与工程学院，广州 510640；

2. 广州有色金属研究院 新材料研究所，广州 510650；

3. IRTES-LERMPS Laboratory, Université de Technologie de Belfort-Montbéliard, Belfort Cedex 90010, France

摘 要：采用磁控溅射在大气等离子喷涂的 ZrO_2−7%Y_2O_3(7YSZ)热障涂层表面制备一层厚度约 15 μm 铝膜，对镀有铝膜的热障涂层样品在 700、900 °C 分别保温 1 h 和 5 h 进行真空热处理。采用场发射−扫描电子显微镜对经真空热处理前后镀铝热障涂层的微观结构进行表征。采用 X 射线衍射和透射电子显微镜对经真空热处理前后镀铝热障涂层的物相变化进行分析。对等离子喷涂的 7YSZ 原始热障涂层和镀铝真空热处理后的热障涂层进行室温粒子冲刷性能对比。结果表明：镀铝热障涂层经真空热处理后在涂层表面出现疏松表层和致密底层，其成分主要为 α-Al_2O_3，其中致密底层来源于 Al 膜与 ZrO_2 的高温原位反应且该层有较高的显微硬度。此外，冲刷实验后发现镀铝真空热处理后热障涂层的冲刷性能比无镀铝热障涂层有较大的提高。

关键词：热障涂层；ZrO_2−7%Y_2O_3 (7YSZ)；抗冲刷性；原位反应；α-Al_2O_3

(Edited by Xiang-qun LI)